

Tris(oxazoliny)boratomagnesium-Catalyzed Cross-Dehydrocoupling of Organosilanes with Amines, Hydrazine, and Ammonia

James F. Dunne, Steven R. Neal, Joshua Engelkemier, Arkady Ellern, and Aaron D. Sadow*

Department of Chemistry, Iowa State University, Ames, Iowa 50011, United States

Supporting Information

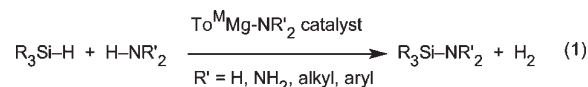
ABSTRACT: We report magnesium-catalyzed cross-dehydrocoupling of Si–H and N–H bonds to give Si–N bonds and H₂. A number of silazanes are accessible using this method, as well as silylamines from NH₃ and silylhydrazines from N₂H₄. Kinetic studies of the overall catalytic cycle and a stoichiometric Si–N bond-forming reaction suggest nucleophilic attack by a magnesium amide as the turnover-limiting step.

Compounds containing Si–N bonds have important applications in synthetic chemistry as bases,¹ silylating agents,² ligands for metal centers, and polymeric precursors for ceramic materials.³ Amines are often protected with tertiary silanes as silazanes,⁴ and amines serve as useful protecting groups in silicon chemistry for the selective conversion of chlorosilanes because the Si–N bond forms readily and is easily transformed into Si–X species (X = halide, alkoxide).⁵ However, the HCl produced and/or basic conditions needed to neutralize the reaction can limit its functional group tolerance, and a stoichiometric equivalent of salt is formed; moreover, chlorosilanes are hydroscopically sensitive and must be stored under carefully controlled conditions. Additionally, the products are controlled only by the substituents on the chlorosilane and the amine partners, limiting control over the selectivity. Catalytic dehydrocoupling of amines and hydrosilanes offers a complementary synthetic method for Si–N bond formation.

Only a few metal-catalyzed cross-couplings of silanes and amines have been described.⁶ Palladium on Al₂O₃ catalyzes the aminolysis of optically active tertiary naphthylphenylmethylsilane with inversion of the silicon stereocenter, while Pd/C gives the racemic product.⁷ Ammonia and the tertiary silazane HN(SiHMe₂)₂ react at 135 °C in the presence of Ru₃CO₁₂ to give polysilazanes and H₂,⁸ while rhodium dimers give mixtures of oligosilazanes from amines and organosilanes.⁹ A chromium catalyst provides Ph₂HSi–NHPh from Ph₂SiH₂ and aniline.¹⁰ Dimethyltitanocene catalyzes the coupling of silanes with ammonia and hydrazine,¹¹ while cuprous chloride catalyzes the coupling of silanes and primary amines.¹² Finally, a number of silazanes have been prepared using [U(NMe₂)₃][BPh₄] as a catalyst.¹³ These few examples show the general challenge of controlling the selectivity, and in addition, there have been few opportunities for direct investigation of the silicon–nitrogen bond-forming steps of these catalytic reactions.

Some of these issues are addressed by the catalytic behavior of the four-coordinate magnesium complex To^MMgMe [To^M = tris(4,4-dimethyl-2-oxazoliny)phenylborate],¹⁴ which we now

report to be an effective precatalyst for the cross-dehydrocoupling of Si–H bonds in organosilanes and N–H bonds in amines to give Si–N bonds and H₂ (eq 1).



With this catalyst system, a range of silazanes can be prepared in high conversion and high yield, as shown in Table 1.

Thus, primary aliphatic amines and anilines are effective coupling partners, and primary and secondary silanes are selective silylating agents. In reactions for which multiple dehydrocoupling steps could give mixtures and oligomers, carefully controlled silane/amine ratios allow the isolation of a single product. Formation of polysilazane, $-\text{[R}'\text{NSiR}_2]_n-$, and poly(aminosilane), $-\text{[SiR(NR}'_2)]_n-$, is not detected. In the absence of To^MMgMe as a catalyst, only starting materials are observed.

The catalytic reaction rates and product identities are noticeably affected by the steric bulk of the organosilane and amine reactants. For example, 3.5 equiv of *n*-PrNH₂ and PhSiH₃ provide the tris(amido)silane (*n*-PrHN)₃SiPh within 15 min (Table 1, entry 1) with To^MMgMe as the catalyst, while *i*-PrNH₂ and PhSiH₃ form only the bis(amido) (*i*-PrHN)₂SiHPh after 45 min at room temperature. Use of excess *i*-PrNH₂ and heating at 100 °C does not afford (*i*-PrHN)₃SiPh. *t*-BuNH₂ requires 24 h for quantitative conversion to monodehydrocoupled *t*-BuHN-SiH₂Ph. Similar effects are observed in To^MMgMe-catalyzed dehydrocoupling of anilines and silanes, as (PhHN)₂SiHPh forms rapidly while the reaction of Ph₂SiH₂ and PhNH₂ requires heating at 60 °C. The more hindered secondary amine Ph₂NH and PhSiH₃ give a 10% yield of Ph₂NSiH₂Ph after 72 h at 110 °C, and *i*-Pr₂NH does not form detectable silazane products in the presence of To^MMgMe after 5 days at 100 °C. The low reactivity of secondary amines likely inhibits polysilazane formation, which would require coupling of disubstituted R'HNSiR₃. Additionally, only starting materials are observed from mixtures of tertiary BnMe₂SiH and Et₃SiH (Bn = CH₂Ph) with primary amines (PhNH₂, *t*-BuNH₂, *i*-PrNH₂, *n*-PrNH₂) under catalytic conditions at 110 °C after 72 h.

The interaction between the tris(oxazoliny)borate ancillary ligand and the magnesium(II) center is not disrupted in the presence of excess primary amine. For example, To^MMgNH*t*-Bu is robust in the presence of 10 equiv of *t*-BuNH₂ (although amine–amide exchange occurs). Therefore, we decided to investigate the reductive silylation of hydrazine as a multiple

Received: August 12, 2011

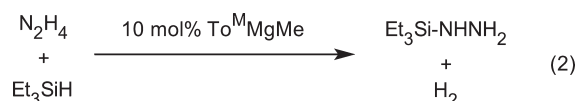
Published: September 29, 2011

Table 1. $\text{To}^{\text{M}}\text{MgMe}$ -Catalyzed Aminolysis of Silanes^a

amine (equiv)	silane	product	% yield (isolated)
<i>n</i> -PrNH ₂ (3.5)	PhSiH ₃	(<i>n</i> -PrHN) ₃ SiPh	99 (99)
<i>n</i> -PrNH ₂ (3)	PhMeSiH ₂	(<i>n</i> -PrHN) ₂ SiMePh	99 (90)
<i>n</i> -PrNH ₂ (0.5)	PhMeSiH ₂	<i>n</i> -PrHNSiHMePh	99 (78)
<i>n</i> -PrNH ₂ (3)	Ph ₂ SiH ₂	(<i>n</i> -PrHN) ₂ SiPh ₂	99 (99)
<i>n</i> -PrNH ₂ (0.5)	Ph ₂ SiH ₂	<i>n</i> -PrHNSiHPh ₂	99 (96)
<i>i</i> -PrNH ₂ (2.5)	PhSiH ₃	(<i>i</i> -PrHN) ₂ SiHPh	99 (99)
<i>i</i> -PrNH ₂ (0.5)	PhSiH ₃	<i>i</i> -PrHNSiH ₂ Ph	99 (45)
<i>i</i> -PrNH ₂ (2)	PhMeSiH ₂	<i>i</i> -PrHNSiHMePh	89 (67)
<i>i</i> -PrNH ₂ (2)	Ph ₂ SiH ₂	<i>i</i> -PrHNSiHPh ₂	99 (97)
<i>t</i> -BuNH ₂ (2.5)	PhSiH ₃	<i>t</i> -BuHNSiH ₂ Ph	99 (90)
<i>t</i> -BuNH ₂ (2)	PhMeSiH ₂	<i>t</i> -BuHNSiHMePh	90 (60)
<i>t</i> -BuNH ₂ (2)	Ph ₂ SiH ₂	<i>t</i> -BuHNSiHPh ₂	99 (81)
PhNH ₂ (2.5)	PhSiH ₃	(PhHN) ₂ SiHPh	99 (97)
PhNH ₂ (2)	PhMeSiH ₂	PhHNSiHMePh	43 ^b (19)
PhNH ₂ (2)	Ph ₂ SiH ₂	PhHNSiHPh ₂	53 ^b (19)

^a Conditions: 5 mol % $\text{To}^{\text{M}}\text{MgMe}$, C_6H_6 , 24 h, room temperature.
^b 60 °C.

NH-containing compound that could undergo one or more dehydrogenative silylations. Remarkably, monosilylhydrazines are accessible from the $\text{To}^{\text{M}}\text{MgMe}$ -catalyzed reactions of N_2H_4 with Et_3SiH , $(\text{C}_3\text{H}_5)_2\text{Me}_2\text{SiH}$, or BnMe_2SiH (eq 2).



$(\text{C}_3\text{H}_5)_2\text{Me}_2\text{SiH}$ reacts quantitatively over 7 h, giving $(\text{C}_3\text{H}_5)_2\text{Me}_2\text{SiNHNH}_2$, whereas BnMe_2SiH and Et_3SiH proceed only to 50% yield after 12 h. The magnesium species $(\kappa^2\text{-To}^{\text{M}})_2\text{Mg}$ was observed in ^1H NMR spectra of micromolar-scale reactions in benzene- d_6 , and this species appears to form from the transient intermediate $\text{To}^{\text{M}}\text{MgNHNH}_2$ as the catalyst decomposition pathway. This intermediate, $\text{To}^{\text{M}}\text{MgNHNH}_2$, forms upon reaction of $\text{To}^{\text{M}}\text{MgMe}$ and N_2H_4 , but attempts to isolate it by evaporation of volatiles afforded mixtures of $\text{H}[\text{To}^{\text{M}}]$ and $\text{To}^{\text{M}}_2\text{Mg}$. $\text{To}^{\text{M}}\text{MgMe}$ also catalyzes reactions of hydrazine with primary and secondary silanes, but mixtures of products are obtained. Still, the monosilylation of hydrazine highlights the impressive selectivity available in these magnesium-catalyzed reactions.

Selective conversion of ammonia is also challenging.¹⁵ The N–H bond is strong (104 kcal/mol)¹⁶ and nonacidic ($\text{pK}_a = 41$ in DMSO).¹⁷ Silylation of ammonia increases the acidity of the remaining NH moieties, potentially increasing their reactivity and making monosilylation difficult. Furthermore, ammonia is a good ligand for metal centers and can shield the (typically Lewis acidic) catalytic site from interactions with other substrates. While this can also be a problem with amines, bulky ancillary ligands sterically inhibit coordination of substituted amines. This strategy is not effective with ammonia because of its small size. The successful reductive silylation of hydrazine and the apparent coordinative saturation of $\text{To}^{\text{M}}\text{MgNHR}$ suggested that the coordination of ammonia would not be an issue. Controlling the extent of silylation might remain a problem, as a monosilylamine is significantly more acidic than ammonia and might be expected to be more reactive. To test our magnesium catalyst for ammonolysis of silanes, excess ammonia was condensed into a storage flask containing BnMe_2SiH , benzene, and 5 mol %

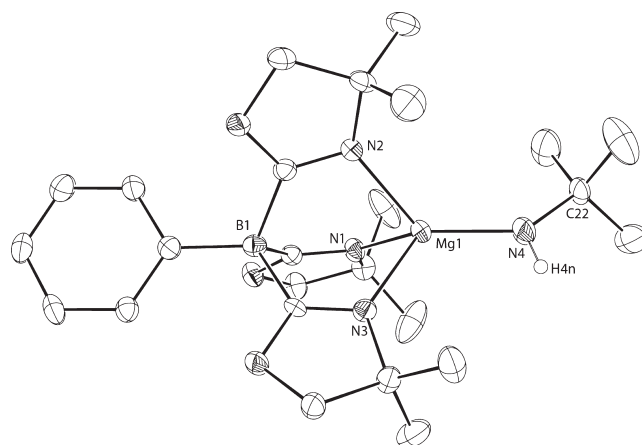
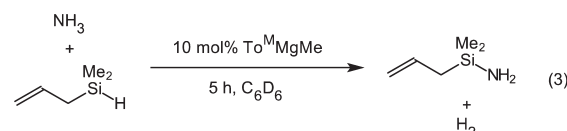


Figure 1. ORTEP diagram of $\text{To}^{\text{M}}\text{MgNHt-Bu}$. Ellipsoids are plotted at 50% probability, and only the H atom bonded to N4 is shown.

$\text{To}^{\text{M}}\text{MgMe}$ (relative to the silane), and the reaction provided $\text{BnMe}_2\text{SiNH}_2$ as the sole product after 15 h. $\text{BnMe}_2\text{SiNH}_2$ was isolated by Kugelrohr distillation (175 °C, 150 mmHg). In the presence of catalytic $\text{To}^{\text{M}}\text{MgMe}$, $(\text{C}_3\text{H}_5)_2\text{Me}_2\text{SiH}$ reacts more rapidly with ammonia than BnMe_2SiH , and quantitative formation of $(\text{C}_3\text{H}_5)_2\text{Me}_2\text{SiNH}_2$ was observed after 5 h in micromolar-scale experiments monitored by ^1H NMR spectroscopy (eq 3).

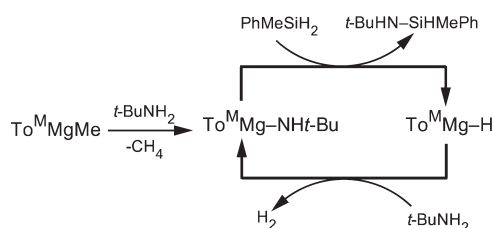


Et_3SiNH_2 , however, requires 15 h for quantitative formation (5 mol % $\text{To}^{\text{M}}\text{MgMe}$, benzene, room temperature). Disilazanes such as $(\text{Et}_3\text{Si})_2\text{NH}$ are not detected by ^1H NMR spectroscopy, in contrast to the case of transition-metal-catalyzed dehydrogenative silylations of ammonia.^{11,12}

Attempts to isolate $\text{To}^{\text{M}}\text{MgNHNH}_2$ or $\text{To}^{\text{M}}\text{MgNH}_2$ as possible intermediates by treatment of $\text{To}^{\text{M}}\text{MgMe}$ with N_2H_4 or NH_3 provided the ligand redistribution product $\text{To}^{\text{M}}_2\text{Mg}$ and unidentified species. Therefore, we focused our mechanistic studies on catalytic aminolysis reactions that are conveniently monitored by ^1H NMR spectroscopy. Spectra of reaction mixtures revealed that H_2 is formed as the dehydrocoupling reactions proceed and that the catalyst resting state is a tris-(oxazolinyl)borate magnesium amide. No other resonances that could be attributed to a $\text{To}^{\text{M}}\text{Mg}$ species were observed in the reaction mixture. These $\text{To}^{\text{M}}\text{MgNHR}$ species ($\text{R} = \text{Pr}$, *i*-Pr, Ph; see below and the Supporting Information for synthesis and characterization) are formed rapidly upon addition of RNH_2 to $\text{To}^{\text{M}}\text{MgMe}$. Over 2 h, $\text{To}^{\text{M}}\text{MgNHt-Pr}$ and $\text{To}^{\text{M}}\text{MgNHn-Pr}$ precipitate from benzene.¹⁸ During independent synthesis, $\text{To}^{\text{M}}\text{MgMe}$ and *t*-BuNH₂ were heated in benzene at 75 °C for 18 h to ensure quantitative formation of $\text{To}^{\text{M}}\text{MgNHt-Bu}$. In this compound, all three oxazoline donors coordinate to magnesium-(II) in the ground state [^{15}N NMR: -158.4 (N-oxazoline) and -117.8 (NHt-Bu); $\nu_{\text{CN}} = 1590 \text{ cm}^{-1}$]; an ORTEP diagram is shown in Figure 1.

In the solid state, $\text{To}^{\text{M}}\text{MgNHt-Bu}$ contains a planar amido group [Mg1-N2-C22 , $137.2(4)^\circ$; Mg1-N4-H4 , $113(6)^\circ$; C22-N4-H4 , $107(6)^\circ$; $\Sigma(\text{X-N-X}) = 357^\circ$] and a four-coordinate magnesium center. Solid-angle analysis revealed that the To^{M} (7.38 sr) and NHt-Bu (2.81 sr) ligands occupy

Scheme 1. Catalytic Cycle for Organosilane Aminolysis

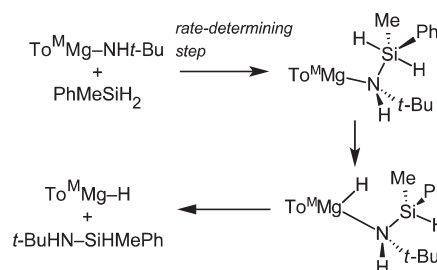


58.8 and 22.4% of the space surrounding the magnesium center, respectively.¹⁹

In catalytic reactions, the consumption of organosilane and the formation of the silazane product are evident from the SiH resonances, which shift downfield as the hydrides are replaced with amides. Additionally, the $^3J_{\text{HH}}$ coupling constants (~ 3 Hz) between the SiH and NH groups give rise to doublet SiH resonances in $\text{RH}_2\text{SiNHR}'$ and triplets in RHSi(NHR')_2 , and therefore, the SiH signal assists in product identification. Furthermore, all of the silazane products in Table 1 are isolable. The in situ concentrations of $\text{To}^{\text{M}}\text{MgNHt-Bu}$, $t\text{-BuNH}_2$, and PhMeSiH_2 in catalytic reactions were monitored by ^1H NMR spectroscopy, and under conditions of excess $t\text{-BuNH}_2$ (17–43 equiv vs PhMeSiH_2) and 20–50 mol % $\text{To}^{\text{M}}\text{MgNHt-Bu}$ at 335 K, the rate law was found to be $-\text{d}[\text{PhMeSiH}_2]/\text{d}t = k'[\text{To}^{\text{M}}\text{MgNHt-Bu}]^1[\text{PhMeSiH}_2]^1[t\text{-BuNH}_2]^0$, with $k' = 0.060(4) \text{ M}^{-1} \text{ s}^{-1}$. This rate law indicates that the turnover-limiting step involves an interaction of the catalyst and PhMeSiH_2 ; $t\text{-BuNH}_2$ is not present in that transition state. As noted above, ^1H NMR spectra of the catalytic reaction mixture suggest that $\text{To}^{\text{M}}\text{MgNHt-Bu}$ is the catalyst resting state. These observations are consistent with the general mechanism shown in Scheme 1, where both steps are irreversible and the interaction of $\text{To}^{\text{M}}\text{MgNHR}$ and the organosilane is turnover-limiting.

Under stoichiometric conditions, isolated $\text{To}^{\text{M}}\text{MgNHt-Bu}$ reacts with hydrosilanes, and this step models Si–N bond formation under catalytic conditions. For example, $\text{To}^{\text{M}}\text{MgNHt-Bu}$ and PhMeSiH_2 (1.4 equiv, -20 to 80°C) react quantitatively to give $t\text{-BuHNSiHMePh}$. A black precipitate forms as the reaction proceeds, and this material is presumed to be the decomposition product from a putative $\text{To}^{\text{M}}\text{MgH}$ species. Linear second-order integrated rate law plots of $\ln\{[\text{PhMeSiH}_2]/[\text{To}^{\text{M}}\text{MgNHt-Bu}]\}$ versus time provided a rate law of $-\text{d}[\text{To}^{\text{M}}\text{MgNHt-Bu}]/\text{d}t = k_{\text{obs}}[\text{To}^{\text{M}}\text{MgNHt-Bu}][\text{PhMeSiH}_2]$, with $k_{\text{obs}}^{273\text{K}} = (3.9 \pm 0.3) \times 10^{-3} \text{ M}^{-1} \text{ s}^{-1}$. The curve obtained from linear regression analysis of a plot of $\ln(k/T)$ versus $1/T$ was used to calculate the second-order rate constant $k_{\text{obs}}^{335\text{K}} = 0.04 \text{ M}^{-1} \text{ s}^{-1}$, which is in reasonable agreement with the rate constant obtained from the catalytic experiments $[0.060(4) \text{ M}^{-1} \text{ s}^{-1}]$.

The activation parameters calculated from a plot of $\ln(k/T)$ versus $1/T$ from -20 to 80°C are $\Delta H^{\ddagger} = 5.9(2) \text{ kcal mol}^{-1}$ and $\Delta S^{\ddagger} = -46.5(8) \text{ cal mol}^{-1} \text{ K}^{-1}$, suggesting a highly ordered transition state.²⁰ A primary kinetic isotope effect of $k_{\text{H}}/k_{\text{D}} = 1.0(2)$ at 0°C was measured for the reaction of $\text{To}^{\text{M}}\text{MgNHt-Bu}$ and PhMeSiD_2 . This small primary isotope effect was essentially temperature-independent from -20 to 80°C , and activation parameters identical to those for PhMeSiH_2 were obtained for PhMeSiD_2 ($\Delta H^{\ddagger} = 5.7(2) \text{ kcal mol}^{-1}$ and $\Delta S^{\ddagger} = -46.1(8) \text{ cal mol}^{-1} \text{ K}^{-1}$). For comparison, kinetic studies of Si–C bond formations mediated by early transition metals and rare-earth elements, which are proposed to involve concerted, four-center transition states (i.e., σ -bond metathesis), have primary

Scheme 2. Proposed Mechanism for $\text{To}^{\text{M}}\text{Mg}$ -Mediated Si–N Bond Formation

isotope effects for Si–C bond formation of ca. 1.1,²¹ highly negative ΔS^{\ddagger} values, and small ΔH^{\ddagger} values that are similar to those for the magnesium-mediated Si–N bond formation.

A few studies probing electronic effects in σ -bond metathesis have shown small changes in rate with electron-donating or electron-withdrawing groups, consistent with small polarization in the transition state.²² Similarly small electronic effects were observed in the $[2\sigma + 2\pi]$ four-center transition state of styrene insertion into Zr-H bonds [$\rho = -0.46(1)$], whereas β -elimination provides a large negative ρ value of $-1.8(5)$ and large KIEs ($k_{\text{H}}/k_{\text{D}} = 3.9\text{--}4.5$).²³ The aryl group is pendent from the β -position of the four-center transition state in both of these transformations.

Second-order rate constants were determined for the reactions of $\text{To}^{\text{M}}\text{MgNHt-Bu}$ and several Ph(aryl)SiH_2 (aryl = Ph, $p\text{-C}_6\text{H}_4\text{F}$, $p\text{-C}_6\text{H}_4\text{Me}$, $p\text{-C}_6\text{H}_4\text{OMe}$, $p\text{-C}_6\text{H}_4\text{CF}_3$).²⁴ The organosilanes with electron-withdrawing groups react more rapidly than those with electron-donating groups. A Hammett plot of $\log(k^{\text{X}}/k^{\text{H}})$ versus σ provides a positive slope ($\rho = 1.4$). Thus, the activation barrier is decreased with electron-withdrawing substituents on silicon. This effect is consistent with a reaction pathway involving a five-coordinate silicon species $\text{To}^{\text{M}}\text{MgHt-BuN-SiPh(aryl)H}_2$ that is stabilized by electron-withdrawing groups. However, the magnitude of the inductive electronic effect is inconsistent with a concerted bond-breaking and bond-forming process; electron-withdrawing groups are expected to have counteracting effects on bond formation and bond cleavage by simultaneously increasing the barrier for hydride transfer to magnesium while stabilizing the five-coordinate silicon center. The temperature-independent primary isotope effect of unity further supports little Si–H bond cleavage in the transition state.

Considering these points, we suggest that these reactions involve nucleophilic attack of the amide on silicon to form a five-coordinate silicon center in the rate-determining step, which is followed by rapid hydrogen transfer to magnesium in a step reminiscent of β -elimination (Scheme 2).

Two additional observations suggest that this mechanism is more reasonable than the concerted four-centered transition-state-like pathway. First, the reaction rate is decreased with the less nucleophilic anilide versus the aliphatic amide, which is consistent with nucleophilic attack playing an important role in the rate-limiting step. Second, a zeroth-order amine concentration dependence was observed in the catalytic rate law even at very high concentrations without evidence of inhibition by amine coordination. Thus, these reactions may be performed even in liquid NH_3 . In contrast, intermolecular σ -bond metathesis reactions require coordinative unsaturation and are inhibited by

coordinating groups.^{22,25} Our hydroamination studies suggest that amines coordinate to the magnesium center in $\text{To}^{\text{M}}\text{MgNHR}$ compounds, either to give a five-coordinate magnesium or substitute an oxazoline.¹⁴ Thus, the zeroth-order amine dependence (rather than an inverse dependence) suggests that an open coordination site is not important in the current Si–N bond formation.

Notably, the nature of nucleophilic substitution at silicon and the role of electrophilic assistance have long been debated, primarily by assessing retention or inversion of stereochemistry in chiral silicon centers.²⁶ In fact, $n\text{-Bu}_4\text{NF}$ catalyzed silane aminolysis is proposed to involve five-coordinate silicon centers without electrophilic assistance.²⁷ Despite the importance of Si–E bond formations ($\text{E} = \text{C}, \text{Si}, \text{O}, \text{N}$) in catalytic chemistry, experimental investigations of electronic effects in d^0 - and f^n -metal-mediated Si–E bond formations are scarce. Thus, we are currently examining the kinetic features of other d^0 - and f^nd^0 -metal-mediated Si–E bond formations to identify the features (coordinative unsaturation, bond polarity, steric constraints, and related effects of ancillary ligands) that influence the mechanism of these types of reactions in order to develop new catalysis.

■ ASSOCIATED CONTENT

S Supporting Information. Experimental procedures, data from kinetic measurements, and crystallographic data (CIF). This material is available free of charge via the Internet at <http://pubs.acs.org>.

■ AUTHOR INFORMATION

Corresponding Author

sadow@iastate.edu

■ ACKNOWLEDGMENT

Financial support for this work was provided by the National Science Foundation (CHE-0955635) and (CRIF-0946687) and the ACS-PRF-Green Chemistry Institute. S.R.N. was supported by a GAANN Fellowship. A.D.S. is an Alfred P. Sloan Fellow.

■ REFERENCES

- (1) As bases: Fieser, L. F.; Fieser, M. *Reagents in Organic Chemistry*; Wiley: New York, 1967.
- (2) As silylation agents: Roth, C. A. *Ind. Eng. Chem. Prod. Res. Dev.* **1972**, *11*, 134. (b) Tanabe, Y.; Murakami, M.; Kitaichi, K.; Yoshida, Y. *Tetrahedron Lett.* **1994**, *35*, 8409. (c) Tanabe, Y.; Misaki, T.; Kurihara, M.; Iida, A.; Nishii, Y. *Chem. Commun.* **2002**, 1628. (d) Iida, A.; Horii, A.; Misaki, T.; Tanabe, Y. *Synthesis* **2005**, *16*, 2677.
- (3) (a) Neugebauer, P.; Jaschke, B.; Klingebiel, U. In *The Chemistry of Organic Silicon Compounds*; Wiley: Chichester, England, 1989; Vol. 3, pp 429–468. (b) Armitage, D. A. In *The Silicon–Heteroatom Bond*; Wiley: Chichester, England, 1991; pp 365–484.
- (4) Wuts, P. G. M.; Greene, T. W. *Protecting Groups in Organic Synthesis*, 4th ed.; Wiley: New York, 2006.
- (5) (a) Eaborn, C. *Organosilicon Compounds*; Butterworths: London, 1960; p 333. (b) Fessenden, R.; Fessenden, J. S. *Chem. Rev.* **1961**, *61*, 361. (c) Passarelli, V.; Carta, G.; Rossetto, G.; Zanella, P. *Dalton Trans.* **2003**, 413.
- (6) Reichl, J. A.; Berry, D. H. *Adv. Organomet. Chem.* **1998**, *43*, 197.
- (7) Sommer, L. H.; Citron, J. D. *J. Org. Chem.* **1967**, *32*, 2470.
- (8) (a) Blum, Y.; Laine, R. M. *Organometallics* **1986**, *5*, 2081. (b) Laine, R. M. *Platinum Met. Rev.* **1988**, *32*, 64. (c) Youngdahl,

K. A.; Laine, R. M.; Kennish, R. A.; Cronin, T. R.; Balavoine, G. A. In *Better Ceramics through Chemistry III*; Brinker, C. J., Clark, D. E., Ulrich, D. R., Eds.; Materials Research Society: Warrendale, PA, 1988; pp 489–495. (d) Chow, W.; Hamlin, R. D.; Blum, Y.; Laine, R. M. *J. Polym. Sci., Part C: Polym. Lett.* **1988**, *26*, 103. (e) Blum, Y. D.; Schwartz, K. B.; Laine, R. M. *J. Mater. Sci.* **1989**, *24*, 1707.

- (9) Wang, W. D.; Eisenberg, R. *Organometallics* **1991**, *10*, 2222.
- (10) Matarasso-Tchiroukhine, E. *J. Chem. Soc., Chem. Commun.* **1990**, 681.
- (11) (a) Liu, H. Q.; Harrod, J. F. *Organometallics* **1992**, *11*, 822. (b) He, J. L.; Liu, H. Q.; Harrod, J. F.; Hynes, R. *Organometallics* **1994**, *13*, 336.
- (12) Liu, H. Q.; Harrod, J. F. *Can. J. Chem.* **1992**, *70*, 107.
- (13) Wang, J. X.; Dash, A. K.; Berthet, J. C.; Ephritikhine, M.; Eisen, M. S. *J. Organomet. Chem.* **2000**, *610*, 49.
- (14) (a) Dunne, J. F.; Fulton, D. B.; Ellern, A.; Sadow, A. D. *J. Am. Chem. Soc.* **2010**, *132*, 17680. (b) Dunne, J. F.; Su, J.; Ellern, A.; Sadow, A. D. *Organometallics* **2008**, *27*, 2399.
- (15) For an in-depth discussion of catalytic reactions of NH_3 , see: Klinkenberg, J. L.; Hartwig, J. F. *Angew. Chem., Int. Ed.* **2011**, *50*, 86.
- (16) Darwent, B. de B. *Natl. Stand. Ref. Data Ser.* **1970**, *31*, 1.
- (17) Bordwell, F. G. *Acc. Chem. Res.* **1988**, *21*, 456.
- (18) Three ν_{CN} bands in the IR spectra suggest $\text{To}^{\text{M}}\text{MgNHPr}$ and $\text{To}^{\text{M}}\text{MgNHPr}$ are not monomeric as solids (see the Supporting Information), although the ^1H NMR spectra of species generated in situ suggest monomeric structures. Precipitated $\text{To}^{\text{M}}\text{MgNHPr}$ and $\text{To}^{\text{M}}\text{MgNHPr}$ are sufficiently insoluble that solution NMR data were not obtained.
- (19) (a) White, D.; Coville, N. J. *Adv. Organomet. Chem.* **1994**, *36*, 95. (b) Guzei, I. A.; Wendt, M. *Dalton Trans.* **2006**, 3991. (c) Guzei, I. A.; Wendt, M. *Solid-G UW-Madison*, WI, 2004.
- (20) (a) Espenson, J. H. *Chemical Kinetics and Reaction Mechanisms*, 2nd ed.; McGraw-Hill: New York, 1995. (b) Morse, P. M.; Spencer, M. D.; Wilson, S. R.; Girolami, G. S. *Organometallics* **1994**, *13*, 1646.
- (21) (a) Gountchev, T. I.; Tilley, T. D. *Organometallics* **1999**, *18*, 5661. (b) Sadow, A. D.; Tilley, T. D. *J. Am. Chem. Soc.* **2005**, *127*, 643.
- (22) Thompson, M. E.; Baxter, S. M.; Bulls, A. R.; Burger, B. J.; Nolan, M. C.; Santarsiero, B. D.; Schaefer, W. P.; Bercaw, J. E. *J. Am. Chem. Soc.* **1987**, *109*, 203.
- (23) Chirik, P. J.; Bercaw, J. E. *Organometallics* **2005**, *24*, 5407.
- (24) Rate constants used in the Hammett plot were determined from second-order integrated rate law plots of $\ln\{[\text{Ph}(\text{XC}_6\text{H}_4)_2\text{SiH}_2]/[\text{To}^{\text{M}}\text{MgNHt-Bu}]\}$ vs ΔG^\ddagger ($\text{X} = \text{OMe}, \text{Me}, \text{H}, \text{F}$) for reactions at 313 K; for $\text{X} = \text{CF}_3$, the rate constant was calculated from an Eyring plot for reactions measured over the range 245–313 K because the rate at 313 K was sufficiently high to require verification.
- (25) Watson, P. L.; Parshall, G. W. *Acc. Chem. Res.* **1985**, *18*, 51.
- (26) Bassindale, A. R.; Taylor, P. G. In *The Chemistry of Organic Silicon Compounds*; Wiley: New York, 1989; Vol. 3, pp 839–892.
- (27) Corriu, R. J. P.; Leclercq, D.; Mutin, P. H.; Planeix, J. M.; Vioux, A. *J. Organomet. Chem.* **1991**, *406*, C1.